

# Investigation of using Polyelectrolytes as an Interlayer on Polymer Solar Cells

Wei-Chih Chen<sup>1</sup>, Yung-Cheng Hsiao<sup>1</sup>, Yi-Chiang Huang<sup>1</sup>, Hsu-Feng Lee<sup>1</sup> and Wen-Yao Huang<sup>1,a</sup>

<sup>1</sup> Department of Photonics, National Sun Yat-sen University, 80424 Kaohsiung, Taiwan, R.O.C.

wayne49914020@gmail.com

**Abstract.** A new approach to improve hole extraction anode interfacial layer by introducing polyelectrolytes in polymer solar cells (PSCs). The polyelectrolytes interfacial layer is prepared simply spin-coating on the ITO substrate. Remarkable improvement in the open-circuit voltage (Voc) and short-circuit current density (Jsc) of the PSCs could be achieved upon the introduction of polyelectrolytes anode interfacial layer. To study the effect of polyelectrolytes anode interfacial layer on the device efficiency. The polyelectrolytes are analyzed, exhibited good thermal stability and high transmittance over 85% in visible light region. According to our experiments and measurements, insertion of polyelectrolytes anode interfacial layer can decrease spatial barriers at the active layer/ITO interfaces, planarize the ITO substrate and modify surface of ITO. The PSCs under the optimized structure of ITO/SA8/P3HT:PCBM/LiF/Al exhibited open-circuit voltage of 0.62 V, short-circuit current density of 7.15 mA/cm<sup>2</sup>, fill factor of 54.84%, and power conversion efficiency of 2.43% at AM 1.5G of 100 mW/cm<sup>2</sup>.

## 1. Introduction

The mixture of two polymer Poly(3,4-ethylenedioxythiophene) (PEDOT) : poly(styrene sulfonate) (PSS) are well-known materials as the hole extraction anode interfacial layer in PSCs[1]. Lithium fluoride that was usually plated on cathode was an inorganic compound. It can enhance electron injection which constitute a coupling layer to improves the polymer/metal contact[2]. The PEDOT :PSS were substituted by polyelectrolytes in our previous work. Two kinds of novel materials were developed to have high solubility in our study. In this work, we applied Two kinds of materials, SA8(Fig. 1a) and SP4c(Fig. 1b), to substitute hole transport layer and electron injection layer.

Kang et al. (2008) reported a buffer layer for a polymer solar cell. Insertion of the PTFE buffer layer at the anode of the ITO/organic interface can significantly improve the Jsc, Voc, and PCE of PSCs[3].

Xu et al. (2013) through a low temperature and inexpensive method of spin-coating a copper acetylacetonate (Cu(acac)<sub>2</sub>) 1,2-dichlorobenzene solution onto ITO. The device with CuO<sub>x</sub> anode buffer layer demonstrated improved PSCs performance compared with PEDOT:PSS anode buffer layer[4].

In our lab previous work, Zhou et al. used a molecular structure, 6F (Fig. 1c), as anode interfacial layer in PSCs[5]. The structure and characteristic have reported in his thesis. Zhu and Zhang et al. utilized a small molecular, 6F, that designed and synthesized two kinds of polymers, SA8 and SP4c, respectively. Both of their structure and characteristic have reported in their thesis, respectively[6,7].



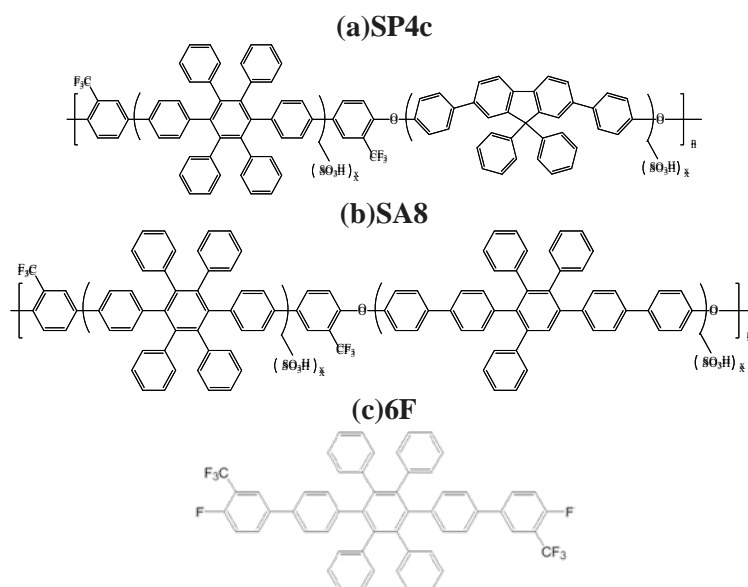


**Figure 1.** Chemical structures of compounds SP4c and SA8 and 6F.

## 2. Experimental

### 2.1. Materials and characterization

The temperature of thermal degradation (Td) was obtained at the point of 5% weight loss by thermal gravimetric analysis (TGA) which was conducted on a Perkin Elmer PYRIS 1. Under nitrogen condition, both of two polymers performed an excellent thermally stable ability. Under a heating rate of  $10^{\circ}\text{C min}^{-1}$ , Td5% was observed of  $298^{\circ}\text{C}$  and  $284^{\circ}\text{C}$  for SA8 and SP4c.

The poly(3-hexylthiophene) (P3HT) : phenyl-C61-butiric acid methyl ester (PCBM) was as an active layer in this study[8-11]. In order to investigate the effect of SA8 and SP4c as the buffer layer, polymer solar cells were fabricated with configuration of ITO/PEDOT :PSS/P3HT :PCBM/SA8 or SP4c or LiF or none/Al[4].

To achieve energy level matched, the work function of SA8 and SP4c were measured to be  $-5.04\text{eV}$  and  $-4.95\text{eV}$ , respectively. Highest occupied molecular orbital (HOMO) of PEDOT :PSS was observed at  $-5.0\text{eV}$  photo-electron spectroscopy(AC-2). Demonstrated energy level of polymers was suitable as anode interfacial layer. HOMO was conducted on a RIKEN KEIKI Surface Analyzer model(AC-2).

A 40 nm thick layer of PEDOT :PSS was spin-coated onto the glass substrates. The morphological stability and film-forming ability of the three samples was observed by atomic force microscopy. The atomic force microscopy images of all the samples was shown in Figure 4.

### 2.2. Device fabrication and testing

PSS indicates that the PEDOT has been doped with polystyrene sulfonic acid in order to enhance the conductivity of the film[12,13]. A PEDOT :PSS-covered ITO anode reduces the operating voltage and increases the device lifetime remarkably, which was attributed to a lower hole injection barrier between ITO and the hole transport layer as well as a smoother surface than bare ITO[14]. Therefore, there have been a lot of reports about improved hole injection[15]. It was interesting that the PEDOT :PSS was substituted by polyelectrolytes. The structure used in this work were ITO/PEDOT :PSS or SA8 or SP4c or none/P3HT :PCBM/ LiF/Al. Then compared with PEDOT :PSS that has a similar work function(Table 1). All manipulations involving air-sensitive experiments were carried out in the nitrogen glove box.

The performances of the solar cells were obtained from J-V characteristics measured using a Keithley 2400 instrument under  $100 \text{ mW cm}^{-2}$  with AM1.5 G[16].

The EQE measurements were performed using solar simulator (Newport 91160A) obtained from National Renewable Energy Laboratory calibrated silicon cell photodiode used as a reference diode.

**Table 1.** Work function of the SP4c 、SA8 、PEDOT:PSS

	SP4c	SA8	PEDOT :PSS
Work function (eV)	4.95	5.04	5.0

### 3. Results and discussions

Since rigid of the polymer material for the backbone of benzene structure has a good thermal stability. According to the information[17,18], the first pyrolysis temperature was about  $200 \sim 400^\circ\text{C}$  with sulfonate group. Then, the second pyrolysis was from about  $400 \sim 600^\circ\text{C}$  by backbone pyrolysis (Fig. 2).

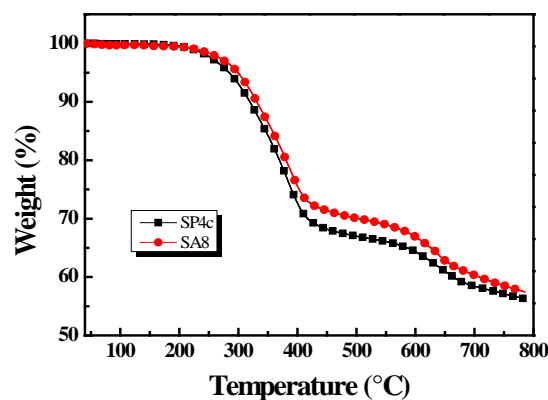


**Figure 2.** TGA curves of the polymers.

Two polymer electrolyte material SP4c, SA8 was dissolved in dimethyl sulfoxide (DMSO) to form a 0.05wt% solution. The device fabrication throughed spin coating a cathode interface layer. The devices structure were displayed in Table 2. The J-V curves characteristic of devices were displayed in Fig 3, related data are shown in Table 3.

**Table 2. The structure of devices.**

Device1 : ITO / PEDOT :PSS / P3HT :PCBM / Al  
 Device2 : ITO / PEDOT :PSS / P3HT :PCBM / SP4c / Al  
 Device3 : ITO / PEDOT :PSS / P3HT :PCBM / SA8 / Al  
 Device4 : ITO / PEDOT :PSS / P3HT :PCBM / LiF / Al

The short-circuit current ( $J_{sc}$ ) of SP4c and SA8 improved from  $6.15 \text{ mA / cm}^2$  to  $7.26 \text{ mA / cm}^2$  and  $8.32 \text{ mA / cm}^2$ (Table 3) , respectively. Compared with lithium fluoride, the open circuit voltage ( $V_{oc}$ ) of SP4c and SA8 can not reach to  $0.62 \text{ V}$ . It can also be seen the characteristics of SP4c and SA8 from the fill factor (FF). They were not improved between the active layer and cathode.

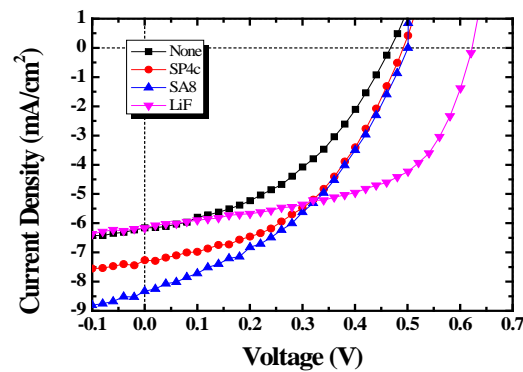


**Figure 3.** J-V curves of the different cathode interfacial layer

**Table 3.** Devices characteristic of PSCs at the different cathode interfacial layer

Cathode interfacial layer	$V_{oc}(V)$	$J_{sc}(mA/cm^2)$	FF(%)	PCE(%)
None	0.46	6.15	43.41	1.23
SP4c	0.50	7.26	45.77	1.66
SA8	0.50	8.32	40.84	1.70
LiF	0.62	6.15	55.48	2.12

In order to confirm that the polyelectrolytes can optimize interface roughness, we scanned surface by the atomic force microscopy. For the roughness of the anode interface layer, the ITO, ITO / PEDOT : PSS, ITO / SP4c, ITO / SA8 Root Mean Square(RMS) roughness value were obtained 4.30, 4.16, 3.83 and 3.13 nm (Table 4), respectively. The SA8 showing a relatively flat surface, 3.13nm, thereby enhanced holes capture, in favor of the active layer spin coating.

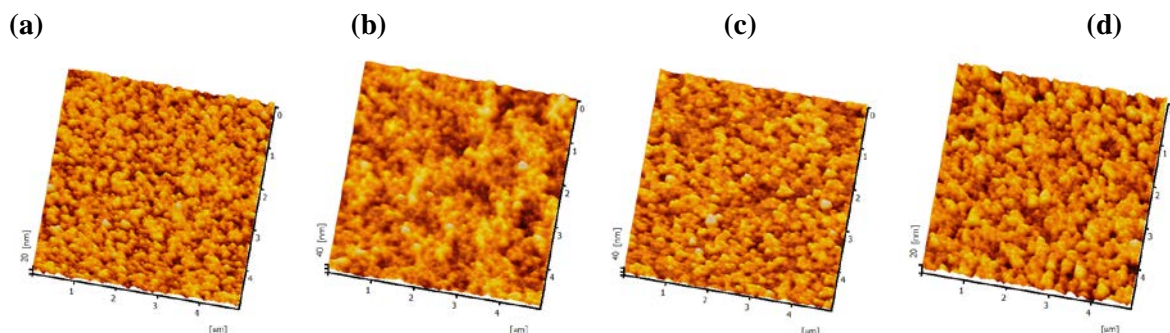


**Figure 4.** AFM images of dimension  $5 \times 5 \mu m$ . (a) ITO、(b) ITO/PEDOT :PSS、(c) ITO/SP4c、(d) ITO/SA8

**Table 4.** The roughness of the different anode interface layer

	ITO	ITO/PEDOT :PSS	ITO/SP4c	ITO/SA8
<b>Ra (nm)</b>	3.51	3.30	3.03	2.53
<b>RMS (nm)</b>	4.30	4.16	3.83	3.13

In this work, Both of SP4c and SA8 have energy level about 5.0eV. Control devices without the presence of the PEDOT :PSS hole transporting layer (Device 1) and devices based on PEDOT :PSS (Device 4) were also fabricated for comparison (Table 5).

**Table 5** The structure of devices.

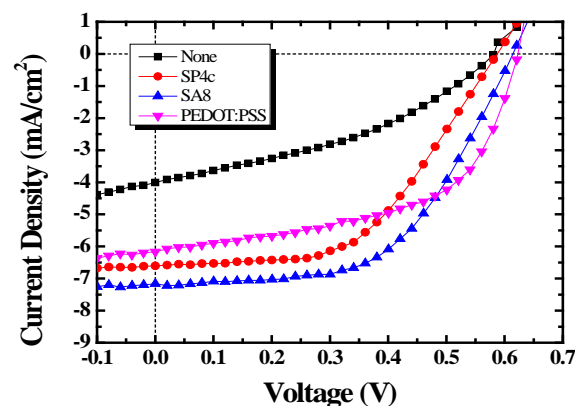
Device1 : ITO / P3HT :PCBM / LiF / Al

Device2 : ITO / SP4c / P3HT :PCBM / LiF / Al

Device3 : ITO / SA8 / P3HT :PCBM / LiF / Al

Device4 : ITO / PEDOT :PSS / P3HT :PCBM / LiF / Al

According to the results depicted in Fig 5. Polymer solar cells (PSCs) reached a maximum short-circuit current ( $J_{sc}$ ) and power conversion efficiency of 2.43% and an external fill factor (FF) of 54.84% was also determined. Such results indicate that, introduced into the polyelectrolytes contribute to improve the efficiency of PSCs.

**Figure 5.** J-V curves of the different anode interfacial layer

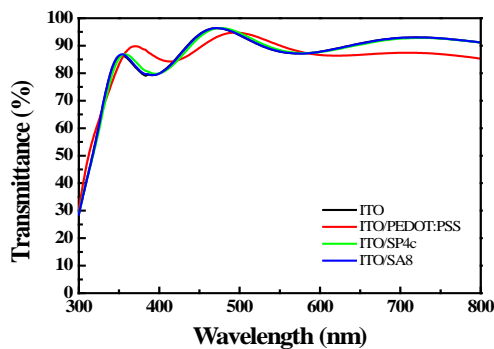
The best performance was achieved in device 3 (Table 6), which showed the short-circuit current ( $J_{sc}$ ) of 7.15mA/cm<sup>2</sup>, the open circuit voltage ( $V_{oc}$ ) of 0.62V (Fig. 5). Enhance the short-circuit current ( $J_{sc}$ ) was attributed to a relatively flat surface, reducing the overall device resistance, resulting ITO surface properties change. Overall, the anode interface layer applied polyelectrolytes to fabricate PSCs device obtained good results.

Anode interfacial layer film transmittance was an important condition for the absorption of light. In order to increase the light absorption of the active layer, the anode interfacial layer material must have a low extinction coefficient in the range of visible light wavelength. The transmittance of the spin-coated thin film of polyelectrolytes was measured by the UV-Vis Spectrometer. PEDOT :PSS and polyelectrolytes was observed above 40nm and 10nm, respectively.

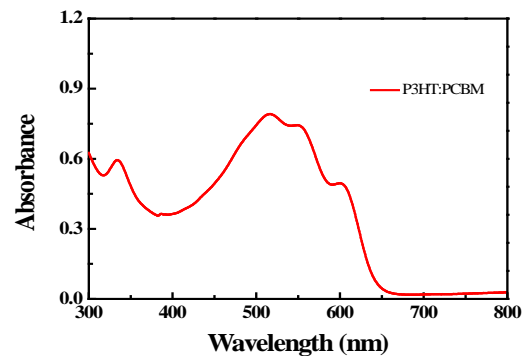
**Table 6.** Devices characteristic of PSCs at the different anode interfacial layer

Anode interfacial layer	$V_{oc}(V)$	$J_{sc}(mA/cm^2)$	FF(%)	PCE(%)
None	0.58	4.02	38.30	0.89
SP4c	0.58	6.60	52.29	2.00
SA8	0.62	7.15	54.84	2.43
PEDOT :PSS	0.62	6.15	55.48	2.12

(a)



(b)

**Figure 6.** UV-vis spectrum of the (a) anode interfacial layer (b) active layer

The transmittance of all the samples was shown in Figure 6(a). It demonstrated polyelectrolytes was different from PEDOT :PSS advantage on transmittance. In addition, we measured the absorption spectra of the active layer was shown in Figure 6(b).

To further understand the impact of polymer on ITO, contact angle measurement was a useful system. Anode interface layer surface energy can be calculated by liquid contact angle, and explained hydrophilicity. In this work, deionized water and diiodomethane was dropped to make the contact angle measurements. For deionized water, the PEDOT :PSS, SP4c, SA8 exhibited contact angle of  $40.9^\circ$ ,  $28.1^\circ$ ,  $20.8^\circ$ , respectively. For diiodomethane, the PEDOT :PSS, SP4c, SA8 exhibited contact angle of  $30.1^\circ$ ,  $35.4^\circ$ ,  $35.7^\circ$ , respectively. The surface free energy of the PEDOT :PSS, SP4c, SA8 was  $63.7$ ,  $68.6$ ,  $73.3 \text{ mJ/m}^2$ , respectively. This result was consistent with the function of the sulfonate group. It was attributed to the increase in chemical polarity and enhanced surface free energy. The difference was reflected in efficiency.

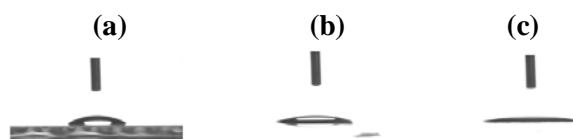


**Figure 7.** Deionized water of contact angles formed by sessile liquid drops on (a)PEDOT:PSS (b)SP4c (c)SA8

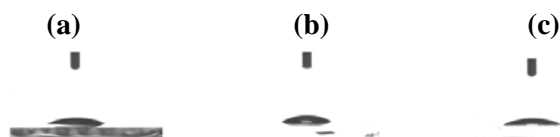


**Figure 8.** Diiodomethane of contact angles formed by sessile liquid drops on (a)PEDOT:PSS (b)SP4c (c)SA8

#### 4. Conclusions

In this paper, SA8 has such excellent thermal stability and morphological stability. The polyelectrolytes material is formed an anode interface layer by spin coating. The polyelectrolytes, SA8, was dissolved in dimethyl sulfoxide (DMSO) production element and was made polymer solar cells device. The short-circuit current ( $J_{sc}$ ) was obtained of  $7.15\text{mA}/\text{cm}^2$  at AM 1.5G of  $100\text{mW}/\text{cm}^2$ , higher than devices based on PEDOT:PSS. The fill factor of 54.84%, and power conversion efficiency of 2.43% can be achieved.

#### References

- [1] R. Po, C. Carbonera, A. Bernardi and N. Camaioni, *Energy Environ. Sci.*, **4**, 285–310 (2011).
- [2] S. E. Shaheen, G. E. Jabbour, M. M. Morrell, Y. Kawabe, B. Kippelen, N. Peyghambarian, M.-F. Nabor, R. Schlaf, *Appl. Phys. Lett.*, **84**, 2324 (1998)
- [3] Kang, Bonan, L. W. Tan, and S. R. P. Silva. *Appl. Phys. Lett.* **93**, 133302, (2008).
- [4] Q. Xu, F. Wang, Z. Tan, L. Li, S. Li, X. Hou, G. Sun, X. Tu, J. Hou and Y. Li, *ACS Appl. Mater. Interfaces*, **5**, 10658–10664, (2013).
- [5] Y. H. Zhou (2015). Investigation of using multi-fluoro monomers as buffer layer on organic solar cells. Unpublished master's thesis, National Sun Yat-sen University, Kaohsiung.
- [6] M. H. Zhu (2012). Synthesis and Application of Poly(arylene ether)s for Proton Exchange Membrane. Unpublished master's thesis, National Sun Yat-sen University, Kaohsiung.
- [7] J. X. Zhang (2013). The effect of substitute numbers of benzene ring on the proton conductivity of alternative sulfonated poly(arylene ether)s. Unpublished master's thesis, National Sun Yat-sen University, Kaohsiung.
- [8] G. Li, V. Shrotriya, Y. Yao and Y. Yang, *J. Appl. Phys.*, **98**, 043704 (2005).
- [9] G. Li, V. Shrotriya, J. Huang, Y. Yao, T. Moriarty, K. Emery and Y. Yang, *Nature Materials*, **4**, 864–868 (2005).
- [10] W. Ma, C. Yang, X. Gong, K. Lee and A. J. Heeger, *Adv. Funct. Mater.*, **15**, 1617–1622 (2005)
- [11] R. He, L. Yu, P. Cai, F. Peng, J. Xu, L. Ying, J. Chen, W. Yang and Y. Cao, *Macromolecules*, **47**, 2921–2928 (2014).
- [12] T. M. Brown, J. S. Kim, R. H. Friend, F. Cacialli, R. Daik and W. J. Feast, *Appl. Phys. Lett.*, **75**, 1679–1681 (1999).
- [13] Vosgueritchian, Michael, Darren J. Lipomi, and Zhenan Bao. *Adv. Funct. Mater.* **22**, 421 (2012).
- [14] F. Zhang, A. Petr, H. Peisert, M. Knupfer and L. Dunsch, *J. Phys. Chem. B*, **108**, 17301–17305 (2004).
- [15] R. Kang, S. Oh and D. Kim, *ACS Appl. Mater. Interfaces*, **6**, 6227–6236 (2014).
- [16] D. G. Collins, W. G. Blattner, M. B. Wells and H. G. Horak, *Applied Optics*, **11**, 2684–2696 (1972).

- [17] H. Y. Jung, K.Y. Cho, K. A. Sung, W. K. Kim and J. K. Park, *J. Power Sources*, 163, 56–59 (2006).
- [18] H. Y. Jung, K. Y. Cho, K. A. Sung, W. K. Kim, M. Kurkuri and J. K. Park, *Electrochimica Acta*, 52, 4916–4921 (2007).